

## CrAlN과 CrZrN의 산화

### Oxidation of CrAlN and CrZrN Films

김민정<sup>a</sup>, 김슬기<sup>a</sup>, 이상율<sup>b</sup>, 이동복<sup>a</sup>

<sup>a</sup>성균관대학교 신소재공학과(E-mail:abc1219@hanmir.com)

<sup>b</sup> 한국한공대학교 재료공학과

**초 록:** Films of CrAlN and CrZrN were deposited on a steel substrate by closed field unbalanced magnetron sputtering, and their oxidation behaviors were investigated. CrAlN films consisted of dense, polycrystalline CrN and AlN fine columns. The formed oxides consisted primarily of crystalline Cr<sub>2</sub>O<sub>3</sub> incorporated with Al<sub>2</sub>O<sub>3</sub>. The oxide layers were thin and compact so as to make CrAlN films more protective than CrN films. In case of CrZrN films, Zr atoms were dissolved in the CrN phase. Zr atoms advantageously refined the columnar structure, reduced the surface roughness, and increased the micro-hardness. However, the addition of Zr did not increase oxidation resistance, mainly because Zr was not a protective element. All the deposited films displayed relatively good oxidation resistance, owing to the formation of the highly protective Cr<sub>2</sub>O<sub>3</sub> on their surface. The Cr<sub>40</sub>Zr<sub>9</sub>N and Cr<sub>31</sub>Zr<sub>16</sub>N films oxidized to Cr<sub>2</sub>O<sub>3</sub> as the major phase and α-ZrO<sub>2</sub> as the minor one, whereas the CrN film oxidized to Cr<sub>2</sub>O<sub>3</sub>.

#### 1. 서론

Chromium nitride (CrN) films are widely used to increase the service life of cutting tools, die molds and machine components, because of their high hardness, good adhesion to most substrate materials, and superior resistance to wear and corrosion. However, they are inevitably degraded by oxidation during service at high temperatures [1-4]. CrN oxidizes via a progressive displacement of nitrogen by oxygen and the formation of Cr<sub>2</sub>O<sub>3</sub>. The oxidation limit of CrN film is commonly known to be about 750 °C. In order to further improve mechanical properties and thermal stability of CrN films, CrAlN and CrZrN films were developed. In this study, CrAlN and CrZrN films were deposited on a steel substrate by closed field unbalanced magnetron sputtering. This study aims to investigate the oxidation behavior of CrAlN and CrZrN films at 800-900 °C in air. The oxidation mechanism was proposed by performing the Au-marker test. Transmission electron microscopic (TEM) analyses were performed to investigate the scale morphology, because such studies were not adequately performed before.

#### 2. 본론

CrAlN and CrZrN films were deposited on tool steels by closed field unbalanced magnetron sputtering with vertical magnetron sources of (Cr+Al) or (Cr+Zr) targets (99.99 % purity) in an (Ar+N<sub>2</sub>) atmosphere. Oxidation tests on the films were carried out at 800 °C and 900 °C for up to 20 h in atmospheric air. Following oxidation, the films were inspected by FE-SEM, XRD, XPS, AES, and TEM.

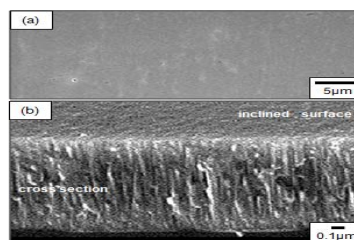


Fig. 1. SEM images of the deposited CrAlN film. (a) top view, (b) fractography.

Fig. 1 shows the SEM images of the as-deposited CrAlN film. The top view displays a featureless, smooth film

surface (Fig. 1(a)). The fracture surface indicates that the film with a columnar structure was dense, adherent, and approximately 1.2  $\mu\text{m}$  thick (Fig. 1(b)).

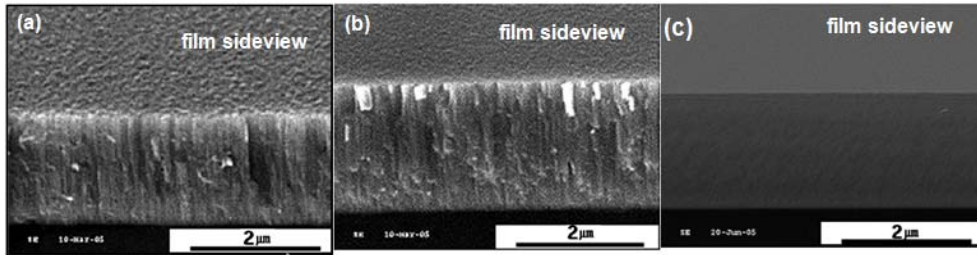


Fig. 2. SEM fracture surfaces of the deposited films. (a) CrN, (b) Cr<sub>40</sub>Zr<sub>9</sub>N, (c) Cr<sub>31</sub>Zr<sub>16</sub>N.

Fig. 2 shows SEM fracture surfaces of deposited films. The CrN film had a typical columnar microstructure with  $\sim 100$  nm in width (Fig. 2(a)). As the Zr content increased, the width of each column decreased, and a more compact microstructure was obtained (Fig. 2(b)). With a further increase in the Zr content, the columnar microstructure was no longer visible, and a dense, compact microstructure was obtained (Fig. 2(c)).

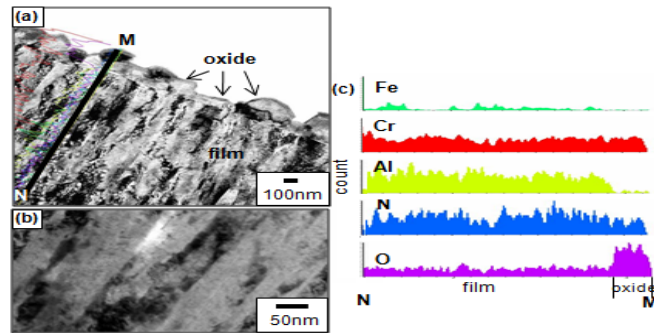


Fig. 3. TEM/EDS analytical results of the CrAlN film after oxidation at 800 °C for 20 h in air. (a) cross-sectional bright field image, (b) enlarged film image, (c) line profiles of Cr, Al, Fe, nitrogen, and oxygen.

Fig. 3(a) shows the TEM image of the partially oxidized CrAlN film. Even after oxidation at 800 °C for 20 h, the scale thickness was only 0.15  $\mu\text{m}$ , reflecting excellent oxidation resistance of the film. The unoxidized film had a dense, polycrystalline structure with fine columns whose width was tens of nanometer (Fig. 3(b)). The EDS line profiles shown in Fig. 3(c) indicate that the scale consisted primarily of Cr<sub>2</sub>O<sub>3</sub>, where a small amount of Cr and Fe dissolved. Nitrogen existed up to the thin oxide scale.

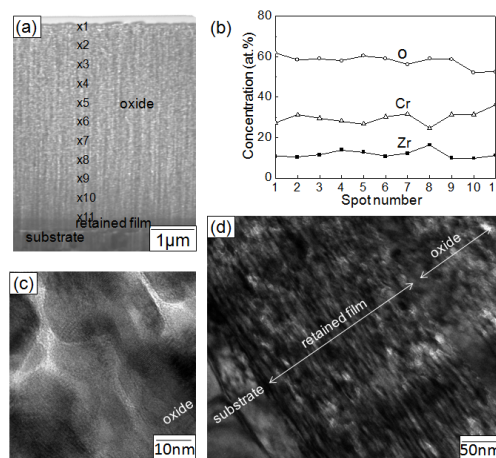


Fig. 4. TEM analysis on the Cr<sub>31</sub>Zr<sub>16</sub>N film after oxidation at 800C for 60 h. (a) cross-sectional image, (b) EDS concentration profiles along point 1-11, (c) high-resolution image of the oxide scale, (d) image of the oxide scale, the retained film, and the substrate .

Fig. 4 shows the TEM/EDS results of the  $\text{Cr}_{31}\text{Zr}_{16}\text{N}$  film after oxidation at  $800^\circ\text{C}$  for 60 h. The TEM image shown in Fig. 4(a) indicates that most of the film oxidized owing to increased oxidation temperature. The original film had a columnar microstructure with  $\sim 65$  nm in width. In Fig. 4(b), no nitrogen was detected. In the oxide scale,  $\text{Cr}_2\text{O}_3$  and  $\text{ZrO}_2$  were uniformly distributed. This confirmed that CrZrN films oxidized by predominant inward diffusion of oxygen. Oxygen can diffuse inward via oxygen-deficient  $\text{ZrO}_2$ . Throughout the oxide scale, no selective oxidation of Cr or Zr occurred. The oxidation of CrN to  $\text{Cr}_2\text{O}_3$  and that of ZrN to  $\text{ZrO}_2$  yield 130% and 141% volume expansion, respectively. Hence, the coexistence of  $\text{Cr}_2\text{O}_3$  and  $\text{ZrO}_2$ , and the partial dissolution of  $\text{ZrO}_2$  in  $\text{Cr}_2\text{O}_3$  could result in a large volume expansion. This volume expansion would be alleviated by volume shrinkage owing to nitrogen escape from the film into the air during oxidation. Nevertheless, the scales formed on CrZrN films were dense. Fig. 4(c) shows that the formed oxide scale consisted of ellipsoidal polycrystallites, along the grain boundaries of which oxygen could diffuse inward. The oxide scale morphology resembled the original film morphology, as shown in Fig. 4(d). The growth of  $\text{Cr}_2\text{O}_3$  and  $\text{ZrO}_2$  crystallites was restricted mainly because of their competitive nucleation and growth. It is seen that the originally columnar structure of the film consisted of nanoalminates aligned parallel with the substrate surface, from Fig. 4(d).

### 3. 결론

CrAlN films displayed superior oxidation resistance due to formation of  $\text{Cr}_2\text{O}_3$  that was incorporated with some amount of  $\text{Al}_2\text{O}_3$ . The thickness of the scales formed was approximately 0.15 and 0.3  $\mu\text{m}$  when the films were oxidized for 20 h in air at 800 and 900  $^\circ\text{C}$ , respectively. The films oxidized via outward diffusion of Cr, nitrogen, and Al, together with inward transport of oxygen. The formed oxide was inevitably  $\text{Cr}_2\text{O}_3$ , where a small amount of Al and Fe ions dissolved, viz.,  $(\text{Cr,Al,Fe})_2\text{O}_3$ .

The CrZrN films consisted of the CrN crystallites, in which Zr dissolved. They always oxidized to  $\text{Cr}_2\text{O}_3$  and  $\alpha$ - $\text{ZrO}_2$ . No nitrogen was detected in the oxide scale, owing to the ensuing outward transport of nitrogen into the air. The oxidation resistance of CrZrN films was largely determined by the presence of the  $\text{Cr}_2\text{O}_3$  scale. Although Zr was less protective than Cr, it densified the oxide scale. The thin  $\text{Cr}_2\text{O}_3$  scale intermixed with  $\alpha$ - $\text{ZrO}_2$  consisted of extremely fine ellipsoidal crystallites.

### 감사의 글

본 연구는 2010년도 지식경제부의 재원으로 한국에너지 기술평가원(KETEP)의 지원을 받아 수행한 연구과제 (전력산업 원천기술 전력선행개발사업; 20101020300460)입니다.

### 참고문헌

1. M. K. Kim, G. S. Kim, and S. Y. Lee, *Met. Mater. Int.* **14**, 465 (2008).
2. K. H. Kim, N. W. Kwak, and S. H. Lee, *Electro. Mater. Lett.* **5**, 83 (2009).
3. A. Aubert, J. Danroc, A. Gaucher, and J. P. Terrat, *Thin Solid Films* **126**, 61 (1985).
4. W. D. Münz and J. Göbel, *Surf. Eng.* **3**, 47 (1987).